FEM SIMULATION FOR DESIGN AND EVALUATION OF AN EDDY CURRENT MICROSENSOR

Heri Iswahjudi and Hans H. Gatzen
Institute for Microtechnology
Hanover University
Callinstrasse 30A, 30167 Hanover
Germany
E-mail: iswahjudi@imt.uni-hannover.de

KEYWORDS
FEM, Eddy Current Sensor, Microsensor, Magnetic Simulation, Coupled Simulation.

ABSTRACT

Proximity measurement and non-destructive material testing by means of the eddy current method was developed originally for large scale measurement. The steadily rising industry demand for distance detection as well as detecting defect in microscale calls for the miniaturization of sensors. Such miniaturization is best achieved by using thin film technology. In this paper, we describe the utilization of the finite element method (FEM) as an analysis tool in the design process of an eddy current microsensor in thin film technology.

INTRODUCTION

Basic Principle

Eddy current sensing is one of the most commonly used non-destructive testing methods. It is based on detecting the interaction of the magnetic fields inducing the eddy currents and the magnetic field created by them. A coil is fed with an alternating current. When bringing it in close proximity of a conductive probe, eddy currents are induced (Fig. 1). Eddy currents are closed loops of induced current circulating in planes perpendicular to the magnetic flux. They normally travel in a plane parallel to the probe's surface. In addition, the magnetic flux associated with the eddy currents opposes the coil's magnetic flux, thereby decreasing the total flux.

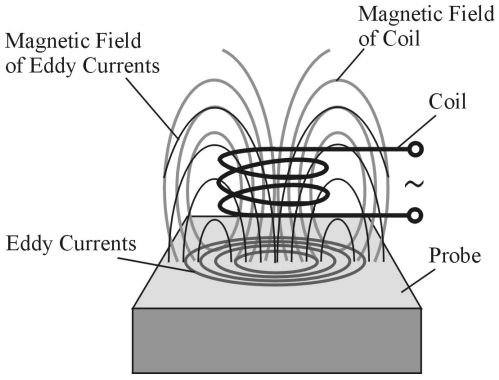

Fig. 1: Basic Principle of Eddy Current Sensing

The distribution of the eddy current in the probe depends on various parameters, e.g. excitation frequency, conductivity and permeability of the probe, distance between sensor and probe, and also presence of a material defect. The last two parameters allow the sensor to be used for distance measurement and material testing. Change in the distribution of eddy currents generates alteration in the total magnetic flux. This provides the basis for extracting information during eddy current testing (McMaster et al. 1986).

Fig. 2 depicts the black-box model of an eddy current sensor. The function of an eddy current sensor can be subdivided into three sub-functions.

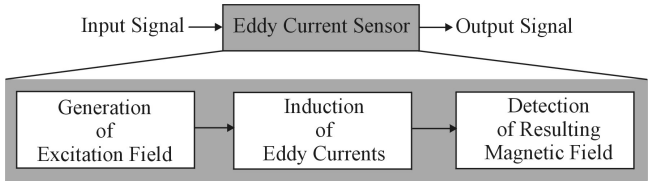

Fig. 2: Functions of an Eddy Current Sensor

The generation of the excitation field is carried out by using a coil fed by an alternating current. Increasing the sensitivity of eddy current measurement can be obtained using a magnetic core, which focuses the magnetic field and restricts the spreading of the magnetic flux away from the region of interest.

There are two basic methods to detect a change of the resulting magnetic field. Using the single coil method, the change of the magnetic field is measured as a change in coil impedance. The second method uses separate coils for excitation and for field pickup. In this approach both coils are magnetically linked. The superposition of magnetic fields generated by the excitation coil and the eddy currents induces a voltage in the pickup coil. Changes in the magnetic field could be measured by evaluating the voltage drop in the pickup coil.

Sensor Miniaturization

To improve a sensor's lateral resolution, the sensor's physical dimensions have to be reduced. One of the most promising approaches in miniaturizing a sensor is bulding it

applying thin film technology. To date, eddy current sensors based on this technology are reported for the applications as proximity sensors, as well as non-destructive testing for cracks and flaws in metals (Gomez et al. 2000; Sadler and Ahn 2001; Yamada et al. 1995).

In this paper, we describe the simulation approach to the design and evaluate an eddy current microsensor as published in Gatzen et al. 2002. The sensor was fabricated in thin film technology, using a combination of electroplating, sputter deposition, and photolithography. For thin film devices, rather expensive photo masks for their fabrication are required. Additionally, the complex physical interaction in the eddy current measurement leads to the utilization of simulation methods as a part of the design process.

Governing Equations

To describe an addy current sensor, the governing equations which derived from Maxwell's equations are:

$$\nabla \times \boldsymbol{H} = \boldsymbol{J}_s + \boldsymbol{J}_e \tag{1}$$

$$\nabla \times \boldsymbol{E} = -\frac{\partial \boldsymbol{B}}{\partial t} \tag{2}$$

$$\nabla \cdot \boldsymbol{B} = 0 \tag{3}$$

where the various quantities involved are the magnetic field $\boldsymbol{H}$, the applied source current density vector $\boldsymbol{J}_s$, the induced eddy current density vector $\boldsymbol{J}_e$, the electric field intensity $\boldsymbol{E}$, and the magnetic flux density $\boldsymbol{B}$. The above field equations are supplemented by a constitutive relation that describes the behavior of electromagnetic materials:

$$\boldsymbol{B} = \mu_r \mu_0 \boldsymbol{H} \tag{4}$$

where μ_r and μ_0 is the relative permeability and the permeability of air, respectively. By introducing the magnetic vector potential $\boldsymbol{A}$ defined as $\boldsymbol{B} = \nabla$ x $\boldsymbol{A}$, we get (Ida 1995):

$$\boldsymbol{E} = -\frac{\partial \boldsymbol{A}}{\partial t} - \nabla V \tag{5}$$

Substituting (5) in (1) with $\boldsymbol{J}_e = \sigma \boldsymbol{E}$ and $\mu = \mu_r \mu_0$ resulting

$$\nabla^2 \boldsymbol{A} = -\mu \boldsymbol{J}_s + \mu\sigma \frac{\partial \boldsymbol{A}}{\partial t} \tag{6}$$

Finite Element Method (FEM)

We used a commercial FEM-software package, ANSYS, to solve the equations with the magnetic vector potential $\boldsymbol{A}$ as primary unknown. Calculations of impedance and induced voltage are the next steps in the simulation. The coil impedance is directly calculated from the magnetic vector (Ida 1995). The general formula for the calculation of impedance of a length of wire carrying a current given as:

$$z = \frac{j\omega}{I} \int_l \boldsymbol{A} \cdot \boldsymbol{dl} \tag{7}$$

In the finite element formulation, if the coil occupies k elements, the impedance per unit length is:

$$z = \frac{j\omega J_s}{I_s^2} \sum_{i=1}^{k} \Delta_i A_{ci} \tag{8}$$

where I is the source current, Δ_i the element cross sectional area in the finite element domain, and A_{ci} the magnetic vector potential within the element. Induced voltage in the coil is determined by:

$$U_{ind} = -j\omega \int_l \boldsymbol{A} \boldsymbol{dl} \tag{9}$$

In finite element formulation with k elements of the coil, Eq. (9) is given as:

$$U_{ind} = -j\omega \sum_{i=1}^{k} \Delta_i A_{ci} \tag{10}$$

PRELIMINARY INVESTIGATION

Sensor Concepts

In a preliminary investigation, the important aspects in designing the sensor were investigated. The technological boundaries in the fabrication process such as the smallest achievable line width and the maximal layer thickness have to be taken into account. Moreover, the sensor performance is affected by the choice of appropriate materials for coils, magnetic core, and insulation layers. The materials chosen for the sensor are listed in Table 1.

Table 1: Materials for the Sensor and Its Properties

	Material	Permeability μ_r	Conductivity σ [m/(Ωmm²)]
Coil	Cu	1	5.81 x 10^1
Magnetic core	NiFe (81%/19%)	1000	1.67

Two alternatives for the sensor design were proposed. The first concept used the change of the coil impedance to detect eddy currents in the probe (Fig. 3 (a)). It featured a seven-turn coil with a cross section of 10 µm x 5 µm and an E-shaped magnetic core. The second concept relied on the detection of induced voltage in the pickup coil (Fig. 3 (b)). Both the resulting designs used identical coil's dimensions.

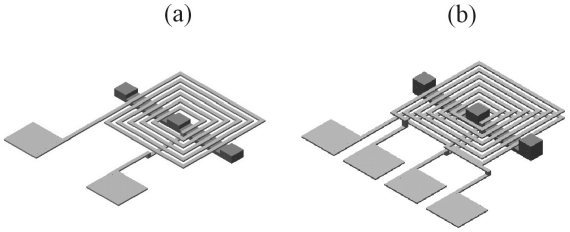

Fig. 3: Alternatives Sensor Designs;
(a) Design 1; (b) Design 2

Sensor Concept Evaluation

The aim in evaluating the sensor concepts was to obtain a basic concept which is suitable for the measurement tasks. Specifically, the investigations were focused on the sensor either being built as a single-coil for impedance measurement or double-coil for detecting induced voltage.

For the application as a proximity sensor, one of the objectives was the design of the sensor with a high sensitivity of detecting a change in the distance between sensor and probe. Therefore, initial simulations in the proximity detection were conducted. As a probe material, stainless steel with a relative magnetic permeability μ_r of 3.75 and an conductivity σ of 2 m/(Ωmm²) was chosen. The sensor's output signal was calculated for a distance at 10 µm, 30 µm, and 50 µm. To properly represent the magnetic interaction between an eddy current sensor and a probe, coupled FEM was applied. While the FEM domain represented the physical structure, the lumped electrical parameter model was used to describe the whole system behavior. An example of coupled FEM simulation for the design concept according to Fig. 3 (b) is given in Fig. 4.

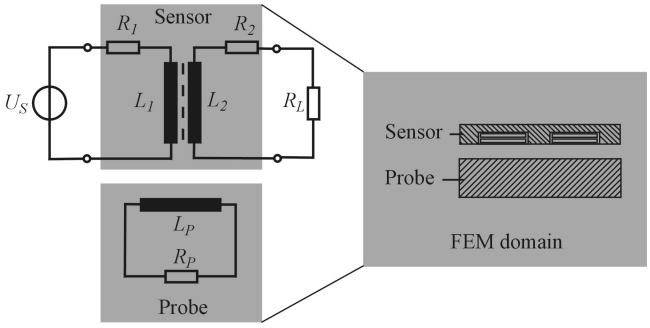

Fig. 4: Coupled FEM Simulation

Fig. 5 presents the simulation result for the coil's impedance of the design concept in Fig. 3 (a). A frequency range from 100 kHz up to 10 MHz was analyzed. As the frequency rose, the impedance change for the given distance increased.

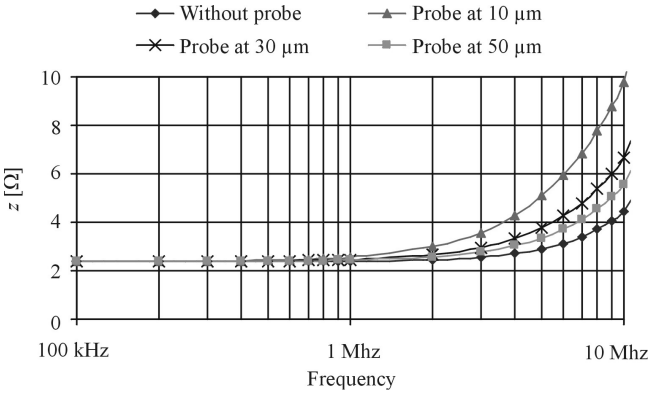

Fig. 5: Calculated Impedance in the Coil of Design 1 in Proximity Detection

The simulation result for the sensor design concept in Fig. 3 (b) is shown in Fig. 6. A higher frequency resulted in higher induced voltage in the pickup coil. The greatest change of the induced voltage occured at a frequency between 1 MHz and 5 MHz.

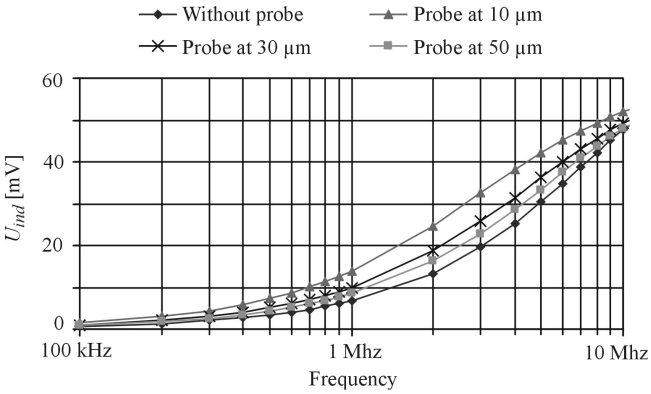

Fig. 6: Calculated Induced Voltage in the Pickup Coil of Design 2 in Proximity Detection

Comparing the simulation results in Fig. 5 and Fig. 6, the output signals of design 2 has typically greater than output signals of design 1. Additionally, the change in the output signals of design 2 for a given change of distance was also higher than design 1. For these reasons, we have chosen the design 2 with the dual-coil approach.

SENSOR DESIGN

Coil and Magnetic Core

In the eddy current measurement, the coil plays an important role. Hence, to achieve high performance of the sensor, an optimal coil design was to be achieved. As mentioned in the introduction (Fig. 2), the coil performs two functions. For generating the excitation field, a high drive current in the coil is desired in order to induce high eddy currents in the probe. Thus, a coil with a great cross section allowing a high drive current is needed. However, to detect the resulting magnetic field, a coil with a high inductance and Q-factor is preferred, achieving a high amplitude of the output signal. The Q-factor describes the relationship between reactive power and power dissipation in the coil and can be expressed with the inductance L and resistance R of the coil as:

$$Q = \frac{\omega L}{R} \tag{11}$$

ω is the angular frequency. It was verified by Ahn and Mark 1998 that the Q-factor is greater for smaller conductor widths where the inductance value is proportional to the square of the coil turns, but the resistance is linearly proportional to the width variation. For optimal coil design, a unique design to fulfill the respective function is required.

Fig. 7 (a) shows the induced eddy currents on the probe surface by a seven-turn excitation coil as described previously. The simulation was conducted for coil system without magnetic core. For comparison, single-turn excitation coil is shown in Fig. 7 (b). The cross section of the single-turn coil was chosen to be 70 µm x 5 µm.

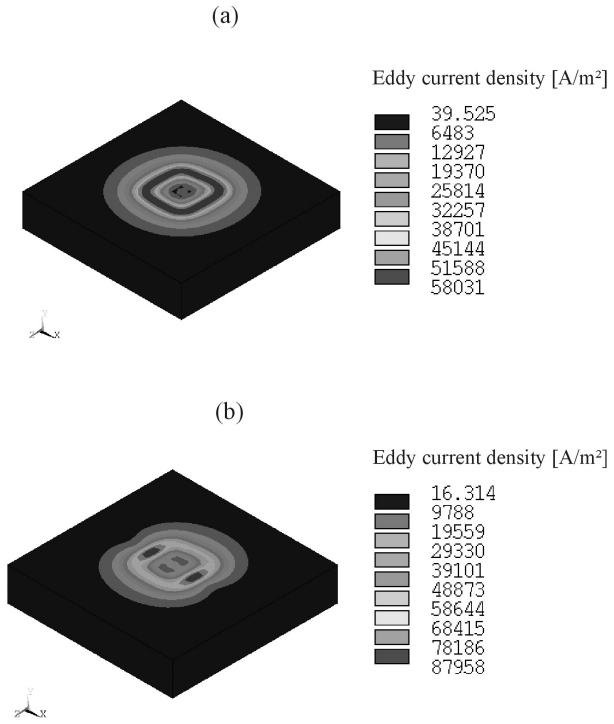

Fig. 7: Comparison of the Induced Eddy Currents on the Probe Surface; (a) Seven-turn Excitation Coil; (b) Single-turn Excitation Coil

The simulation results show that using an excitation coil with a great cross section achieved higher induced eddy currents in the probe. Furthermore, an optimal design of eddy current sensor was best accomplished with appropriate magnetic core focusing the magnetic field. Since the material for the magnetic core is also conductive, eddy current loss taking place in the core had to be considered.

Resulting Sensor Design

Fig. 8 depicts the optimized sensor design. The sensor consisted of a coil system with a single-turn excitation and a seven-turn pickup coil. Furthermore, the sensor featured an E-shaped magnetic core. Its overall size was approx. 700 µm x 450 µm.

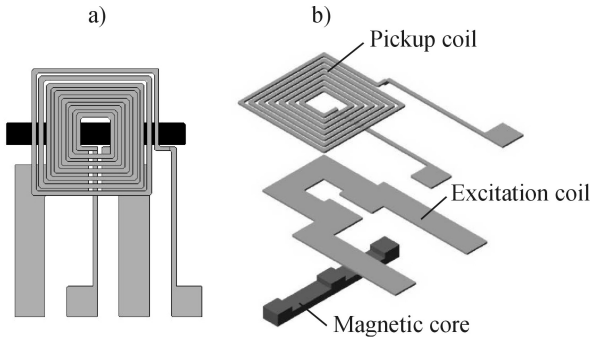

Fig. 8: Optimized Design of the Eddy Current Microsensor; (a) Top View; (b) Exploded View

SENSOR EVALUATION

To characterize the performance of the sensor, a simulation of sensor response in the proximity measurement and in the non destructive testing were conducted.

Proximity Measurement

Fig. 9 depicts the simulation results for proximity measurement in a distance range between sensor and probe of 5 µm - 1 mm. As material for the probe, stainless steel was chosen. The input voltage was set to 20 mV at a frequency of 1 MHz. The amplitude of the induced voltage in the pickup coil decreased with increasing distance. This decrease becomes smaller at the distance up to 200 µm. As a conclusion, the sensor is suitable for proximity measurement in a distance range up to 200 µm.

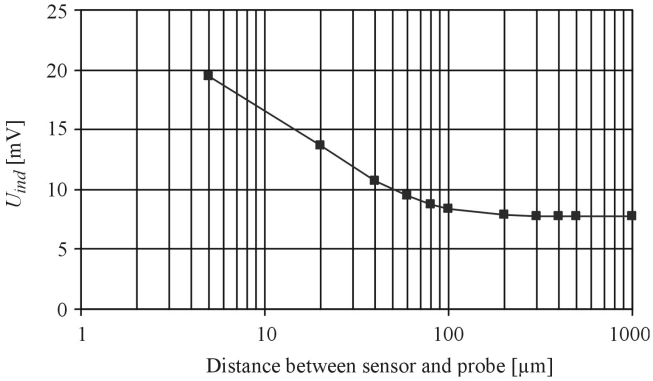

Fig. 9: Induced Voltage as a Function of the Frequency in Proximity Measurement

Probe Material

Eddy current measurement depends on various parameters. Fig. 10 depicts the output signal for stainless steel and copper. The results clearly show that the microsensor is suitable for material detection or material separation.

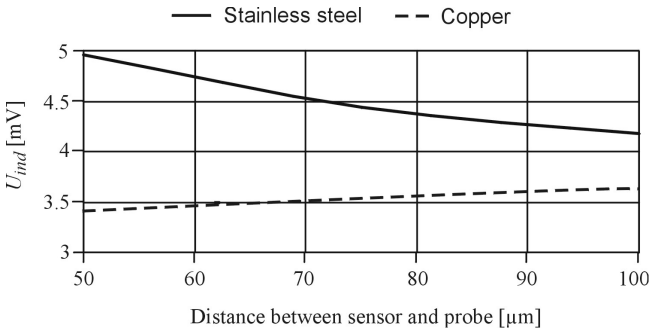

Fig. 10: Influence of the Probe Material

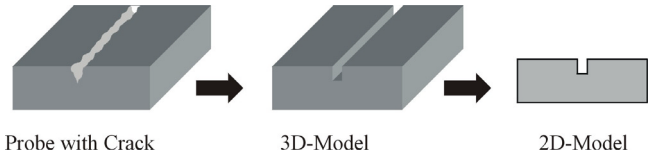

Fig. 11: Crack Modeling

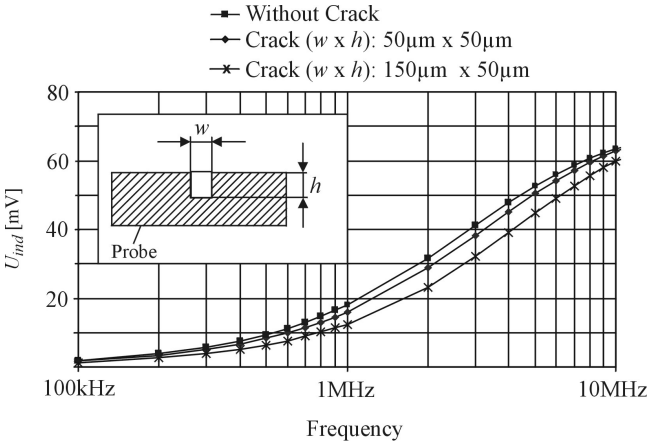

Fig. 12: Simulation for the Probe with Artificial Crack

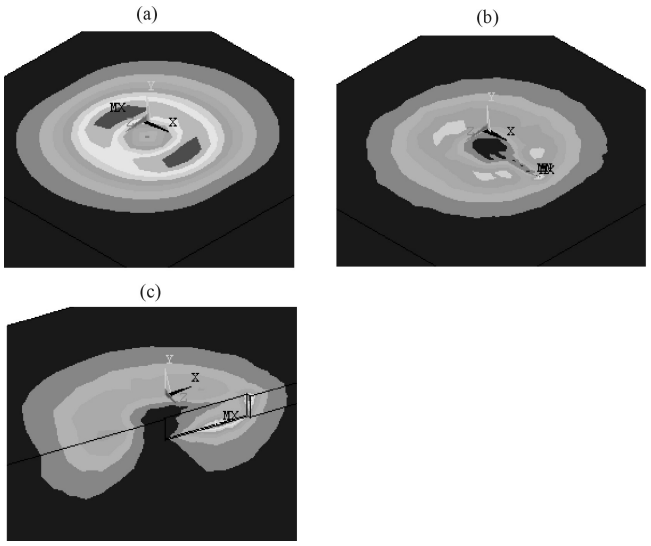

Fig. 13: Distribution of Eddy Currents in the Probe; (a) Without Crack; (b) With Crack; (c) Distribution at the Crack Edge

Non-destructive Testing

For simulating the detection of subsurface damages like microcracks, the conductivity of the finite elements in the region of the crack was assumed to be zero and the relative permeability was chosen equal to the relative permeability of the air ($\mu_r = 1$). Fig. 11 shows the three-dimensional and two-dimensional model of the probe with a microcrack. For non-destructive testing, simulation results in the frequency range of 100 kHz - 10 MHz show that the optimized sensor is able to clearly detect cracks with 50 µm width and 50 µm height on the surface of a stainless steel probe (Fig. 12). Fig. 13 depicts the eddy current distribution in the case of a probe with microcrack. The eddy currents are deformed which results in a change of the induced voltage.

CONCLUSION

In this paper, a thin film based eddy current microsensor for proximity measurement and non-destructive testing of material has been described. The finite element method as analysis tool is well suited for the design process of the sensor leading to a reduction of development cost and time. In the design process, technology limitations were taken into consideration. For the resulting design, simulations to characterize the sensor performance were conducted. In addition, the sensor has been tested as proximity sensor. Initial measurements were in agreement with the developed finite element model. For coil fabricated using thin film techniques, a scaledown of the dimension led to an inductance decrease while the resistance of the coil increases dramatically. As a result, the sensor needs to be operated at high frequencies for which the inductance of the coil dominates its resistance.

REFERENCES

Ahn, C.H. and Mark G.A. 1998. "Micromachined Planar Inductors on Silicon Wafers for MEMS Applications". *IEEE Transactions on Industrial Electronics*, Vol. 45, No. 6, December, pp. 866-876.

Gomez, J.; Esteve, D.; Simonie, J. 2000. "A CMOS Eddy Current Sensor for Microsystems". In *Proceedings of the 3th IEEE International Caracas Conference on Device, Circuits and Systems*, pp. I54/1 – I54/4.

Gatzen, H.H.; E. Andreeva; and H. Iswahjudi. 2002. "Eddy Current Microsensor Based on Thin-film Technology". *IEEE Transactions on Magnetics*, Vol. 38, No. 5, September.

Ida, N. 1995. *Numerical Modeling for Electromagnetic Non-destructive Evaluation*. Chapman & Hall.

McMaster, R.C.; McIntire, P.; Mester, M.L 1986. *Electromagnetic Testing, Nondestructive Testing Handbook*. 2nd ed., Vol. 4, American Society for Nondestructive Testing.

Sadler, D.J. and C.H. Ahn. 2001. "On-chip eddy current sensor for proximity sensing and crack detection". *Sensors and Actuators A*, 91, pp. 340-345.

Yamada, S.; M. Katou; M. Iwahara; and F.P. Dawson. 1995. "Eddy Current Testing Probe Composed of Planar Coils". *IEEE Transaction on Magnetics*, Vol. 31, No. 6, November, pp. 3185-3187.